J. Am. Chem. Soc. **2001,** *123,* 9848−9854

Infrared Spectra of ***cis***- and ***trans***-Peroxynitrite Anion, $OONO^-$, in Solid Argon

Binyong Liang and Lester Andrews*

Contribution from the Department of Chemistry, University of Virginia, P.O. Box 400319, Charlottesville, Virginia 22904-4319

Received June 11, 2001

Abstract: The peroxynitrite anion, of vast importance in biochemistry, is formed in vivo from the reaction of NO and O_2^-. Laser ablation of 10 different metal targets with concurrent 7 K codeposition of NO/Ar and O_2/Ar mixtures gives new metal-independent infrared bands at 1458.3 and 806.1 cm^{-1}, and at 1433.3 and 983.2 cm^{-1}, in addition to known O_4^- and $(NO)_2^-$ absorptions. The new bands are not observed with CCl_4 added to capture electrons or in O_2 and NO experiments without laser ablation to produce electrons, which identifies new product anions. Based on ^{15}NO and $^{18}O_2$ isotopic shifts, splitting patterns in mixed isotopic experiments, and comparison with DFT isotopic frequency calculations, the former absorptions are assigned to ***cis***-$OONO^-$, and the latter pair to ***trans***-$OONO^-$, which are isolated from metal cations trapped elsewhere in the matrix. The ***cis***- and ***trans***-peroxynitrite anion isomers are probably formed via the ion−molecule reaction between O_2^- and NO: the O_2^- anion, made by the capture of ablated electrons, is attested by the observation of O_4^-. ***cis***- and ***trans***-$OONO^-$ are reversibly photoisomerized by visible and near-UV radiation. Collisional stabilization of the $OONO^-$ ion−molecule dimer complex during formation of the solid argon matrix appears to be crucial.

Introduction

Nitrogen oxides are among the most studied and fascinating molecules in chemistry because they are not only byproducts of fuel combustion but, more importantly, are involved in a large number of biological processes, either as benefactors[1] or as unwanted toxic species.[2] In biological systems, it is believed that nitric oxide (NO), which is formed enzymatically, can react with superoxide (O_2^-) to form an exceptional oxidant, peroxynitrite anion ($OONO^-$).[3−5] Peroxynitrite formed by ultraviolet irradiation of nitrate in the Martian soil may account for the initially promising signs of life during the Viking mission.[6] Peroxynitrous acid (HOONO) is also a highly toxic acid and acts as a mediator of free-radical toxicity. It oxidizes proteins and nonprotein sulfhydryls, membrane phospholipids, and DNA.[7,8] As a matter of fact, thousands of papers can be found using “peroxynitrite” as the keyword in the literature search, and most of them are in medical journals.[9]

The chemistry of peroxynitrite has also attracted considerable interest as over thirty papers in this journal since 1994 focus on peroxynitrite. These papers include the role of conformation, carbon dioxide reaction, mechanistic studies, nitration reactions, oxidation of C−H bonds, nitrosation reactions, and peroxynitrite isomerization by myoglobin, to name some examples.[10−16]

The great importance of $OONO^-$ has inspired a recent flurry of theoretical and spectroscopic studies. Peroxynitrite anion is expected to exist in two geometric forms, the cis and trans conformers. Hartree−Fock quantum chemical calculations predicted that the trans form is more stable,[17] and later multiconfiguration self-consistent-field (MCSCF) computations predicted that the cis isomer is slightly more stable, but the trans conformer lies only 0.5 kcal/mol higher.[18] A detailed theoretical study of peroxynitrite reported Hartree−Fock, second-order perturbation theory (MP2), coupled-cluster singles and doubles (CCSD), and density functional theory (DFT) calculations on both cis and trans conformers.[19] This study finds that ***cis***-$OONO^-$ is more stable than ***trans***-$OONO^-$ by 3−4 kcal/mol. A recent X-ray structure analysis concludes that tetramethylammonium peroxynitrite crystallizes in the cis form.[20]

---

[1] Palmer, R. M. J.; Ferrige, A. G.; Moncada, S. *Nature* **1987**, *327,* 524.

[2] Beckman, J. S. *J. Dev. Physiol.* **1991**, *15*, 53.

[3] Huie, R. E.; Padmaja, S. *Free Radical Res. Commun.* **1993**, *18,* 195.

[4] Goldstein, S.; Czapski, G. *Free Radical Biol. Med.* **1995**, *19,* 505.

[5] Pryor, W. A.; Squadrito, G. L. *Am. J. Physiol.* **1995**, *268,* L699 (Lung Cell. Mol. Physiol. 12). Squadrito, G. L.; Pryor, W. A. *Free Radical Biol. Med.* **1998**, *25,* 392.

[6] Plumb, R. C.; Tantayanon, R.; Libby, M.; Xu, W. W. *Nature* **1989**, *338,* 633.

[7] Radi, R.; Beckman, J. S.; Bush, K. M.; Freeman, B. A. *J. Biol. Chem.* **1991**, *266,* 4244.

[8] King, P. A.; Anderson, V. E.; Edwards, J. O.; Gustafson, G.; Plumb, R. C.; Suggs, J. W. *J. Am. Chem. Soc.* **1992**, *114,* 5430.

[9] For example: (a) Muriel, P.; Sandoval, G. *J. Appl. Toxicol.* **2000**, *20,* 435. (b) Cai, L.; Klein, J. B.; Kang, Y. J. *J. Biol. Chem.* **2000**, *275,* 38957.

[10] Tsai, J. H. M.; Harrison, J. G.; Martin, J. C.; Hamilton, T. P.; van der Woerd, M.; Jablonsky, M. J.; Beckman, J. S. *J. Am. Chem. Soc.* **1994**, *116*, 4115.

[11] Lymar, S. V.; Hurst, J. K. *J. Am. Chem. Soc.* **1995**, *117*, 8867.

[12] Houk, K. N.; Condroski, K. R.; Pryor, W. A. *J. Am. Chem. Soc.* **1996**, *118*, 13002.

[13] Uppu, R. M.; Pryor, W. A. *J. Am. Chem. Soc.* **1999**, *121*, 9738.

[14] Shustov, G. V.; Spinney, R.; Rauk, A. *J. Am. Chem. Soc.* **2000**, *122*, 1191.

[15] Uppu, R. M.; Squadrito, G. L.; Bolzan, R. M.; Pryor, W. A. *J. Am. Chem. Soc.* **2000**, *122*, 6911.

[16] Herold, S.; Matsui, T.; Watanabe, Y. *J. Am. Chem. Soc.* **2001**, *123,* 4085.

[17] Koppenol, W. H.; Klasinc, L. *Int. J. Quantum Chem. Biol. Symp.* **1993**, *20*, 1.

[18] Krauss, M. *Chem. Phys. Lett.* **1994**, *222*, 513.

[19] Tsai, H. H.; Hamilton, T. P.; Tsai, J. H. M.; van der Woerd, M.; Harrison, J. G.; Jablonsky, M. J.; Beckman, J. S.; Koppenol, W. H. *J. Phys. Chem.* **1996**, *100*, 15087.

10.1021/ja0114299 CCC: $20.00

Despite numerous kinetic experiments with reactions involving peroxynitrite anion in aqueous solution,[21] spectral identification of these conformers is not well established. In aqueous solution, a broad absorption at 302 nm is ascribed to $OONO^-$.[22,23] When solid nitrates are irradiated at 254 nm, $OONO^-$ is reportedly produced,[24] but no information was deduced about conformation. The Raman spectrum of $OONO^-$ in aqueous alkaline solutions reveals bands at 375, 642, 791, 931, 999, and 1564 cm^{-1}, which are assigned to ***cis***-$OONO^-$ based on the ^{15}N isotopic substitution and CCSD calculation.[10] In an important spectroscopic study, 193-nm irradiation of potassium nitrate (KNO_3) molecules isolated in solid argon at 13 K produced both ***cis***- and ***trans***-potassium peroxynitrite species (K^+)($OONO^-$).[25] The ***cis***-KOONO isomer absorbs at 1444.5, 952.3, 831.6, and 749.1 cm^{-1}, whereas ***trans***-KOONO absorbs at 1528.4, 987.4, and 602.2 cm^{-1}. Similar conformers have also been reported for the lithium and sodium counterparts, with as much as 52-cm^{-1} difference in their infrared absorptions.[25]

In addition to the extensive biological and chemical importance of $OONO^-$, there is considerable interest in gas-phase ion−molecule reactions involving NO^- and O_2^-.[26−35] Although extensive investigations of O_4^- and $(NO)_2^-$ have been performed,[29−35] we have found no evidence for the gaseous $OONO^-$ ion−molecule complex.

Laser ablation of metal targets is known to produce electrons and cations.[36−41] This technique coupled with matrix isolation has been used to produce and characterize small anions in this laboratory, notably O_4^- and $(NO)_2^-$.[36,37,42−44] Here we present a spectroscopic characterization of the isolated ***cis***- and ***trans***-peroxynitrite anions, which are prepared in the straightforward reaction of NO and O_2^- in excess argon.

Experimental and Theoretical Methods

The laser ablation, matrix isolation methods and apparatus have been described in detail previously,[45−47] For the current experiment, separate spray-on lines were used to minimize the reaction of NO and O_2 and formation of unwanted NO_2. Such a co-condensation at 7 K gave only a small amount of extra NO_2. The Nd:YAG laser fundamental (1064 nm, 10-Hz repetition rate with 10-ns pulse width) was focused onto rotating metal targets (Al, Fe, In, Li, Ni, Pd, Ru, Tl, Th, Y). Typically, low laser energy (3−5 mJ/pulse) was used, which favored the stabilization of ionic species. Laser-ablated metal atoms, cations, and electrons were codeposited with O_2 (0.2%−1%) and NO (0.5%) in excess argon onto a 7 K CsI window for 1−2 h at 3−4 mmol/h. Nitric oxide (Matheson) and ^{15}NO (MSD Isotopes, 99% ^{15}N) samples were prepared after fractional distillation from a coldfinger. Oxygen (Matheson), $^{18}O_2$ (Yeda), and $^{16}O_2/^{16}O^{18}O/^{18}O_2$ (Yeda) were used as received. Infrared spectra were recorded at 0.5-cm^{-1} resolution on a Nicolet 550 spectrometer with 0.1-cm^{-1} accuracy using a mercury-cadmium-telluride (MCTB) detector down to 400 cm^{-1}. Matrix samples were annealed to allow diffusion and selected samples subjected to irradiation by filtered light from a medium-pressure mercury lamp (Philips, 175 W, $\lambda > 240$ nm) with the globe removed or a tungsten lamp (Wiko, 360 W operated at 25% power, visible, near-IR).

Density functional theory calculations were performed for both ***cis***- and ***trans***-peroxynitrite anions using the Gaussian 98 program[48] and the hybrid B3LYP functional.[49] The 6-311+G(d) basis set was used for both nitrogen and oxygen atoms.[50] Geometries were fully optimized and the vibrational frequencies computed by using analytical second derivatives. The transition-state optimization employed synchronous transit-guided quasi-Newton methods.[51,52]

Results and Discussion

Systematic matrix infrared spectroscopic investigations of laser-ablated metal reactions with O_2/Ar and NO/Ar mixtures and DFT calculations of potential new products will be described.

Th + O_2/Ar and Th + NO/Ar Experiments. Experiments with thorium and O_2 were performed to develop a background since a high yield of O_4^- was observed in recent laser ablation investigations.[36,53] The reaction product infrared absorptions included ThO at 876.4 cm^{-1}, ThO_2 at 787.2 and 735.1 cm^{-1}, and metal-independent bands also present in other metal−oxygen experiments, namely, O_3 at 1039.5 cm^{-1}, O_4^- at 953.8 cm^{-1}, and O_3^- at 803.9 cm^{-1}.[36,54−56] A new band at 653.2 cm^{-1} shifted to 619.6 cm^{-1} with $^{18}O_2$ and gave an oxygen 16/18 isotopic ratio of 1.0543. This isotopic ratio is lower than the

---

(20) Worle, M.; Latal, P.; Kissner, R.; Nesper, R.; Koppenol, W. H. *Chem. Res. Toxicol.* **1999**, *12*, 305.

(21) For example: (a) Papée, H. M.; Petriconi, G. L. *Nature* **1964**, *204*, 142. (b) Hughes, M. N.; Nicklin, H. G. *J. Chem. Soc. A* **1968**, 450. (c) Goldstein, S.; Meyerstein, D.; van Eldik, R.; Czapski, G. *J. Phys. Chem. A* **2000**, *104*, 9712.

(22) Shuali, U.; Ottolenghi, M.; Rabani, J.; Yelin, Z. *J. Phys. Chem.* **1969**, *73*, 3445.

(23) Barat, F.; Gilles, L.; Hickel, B.; Sutton, J. *J. Chem. Soc. A* **1970**, 1982. Benton, D. J.; Moore, P. *J. Chem. Soc. A* **1970**, 3179.

(24) Plumb, R. C.; Edward, J. O. *J. Phys. Chem*. **1992**, *96*, 3245.

(25) Lo, W. J.; Lee, Y. P.; Tsai, J. H. M.; Tsai, H. H.; Hamilton, T. P.; Harrison, J. G.; Beckman, J. S. *J. Chem. Phys.* **1995**, *103*, 4026.

(26) Fehsenfeld, F. C.; Ferguson, E. E.; Schmeltekopf, A. L. *J. Chem. Phys.* **1966**, *45*, 1844.

(27) McFarland, M.; Dunkin, D. B.; Fehsenfeld, F. C.; Schmeltekopf, A. L.; Ferguson, E. E. *J. Chem. Phys.* **1972**, *56*, 2358.

(28) Rinden, E.; Maricq, M. M.; Grabowski, J. J. *J. Am. Chem. Soc.* **1989**, *111*, 1203.

(29) Coe, J. V.; Snodgrass, J. T.; Freidhoff, C. B.; McHugh, K. M.; Bowen, K. H. *J. Chem. Phys.* **1987**, *87*, 4302.

(30) Posey, L. A.; Johnson, M. A. *J. Chem. Phys.* **1988**, *88*, 5383.

(31) Arnold, D. W.; Newmark, D. M. *J. Chem. Phys.* **1995**, *102*, 7035.

(32) De Luca, M. J.; Han, C. C.; Johnson, M. A. *J. Chem. Phys.* **1990**, *93*, 268.

(33) Sherwood, C. R.; Hanold, K. A.; Garner, M. C.; Strong, K. M.; Continetti, R. E. *J. Chem. Phys.* **1996**, *105*, 10803.

(34) Hanold, K. A.; Continetti, R. E. *Chem. Phys.* **1998**, *239*, 493.

(35) Luony, A. K.; Clements, T. G.; Resat, M. S.; Continetti, R. E. *J. Chem. Phys.* **2001**, *114*, 3449.

(36) Chertihin, G. V.; Andrews, L. *J. Chem. Phys.* **1998**, *108*, 6404 and references therein.

(37) Andrews, L.; Zhou, M. F.; Willson, S. P.; Kushto, G. P.; Snis, A.; Panas, I. *J. Chem. Phys.* **1998**, *109*, 177 and references therein.

(38) Liang, B.; Zhou, M. F.; Andrews, L. *J. Phys. Chem. A* **2000**, *104*, 3905.

(39) Zhou, M. F.; Andrews, L. *J. Phys. Chem. A* **2000**, *104*, 3914.

(40) Zhou, M. F.; Andrews, L. *J Chem. Phys.* **1999**, *110*, 2414.

(41) Andrews, L.; Liang, B. *J. Am. Chem. Soc.* **2001**, *123*, 1997.

(42) Andrews, L.; Zhou, M. F. *J. Chem. Phys.* **1999**, *111*, 6036.

(43) Thompson, W. E.; Jacox, M. E. *J. Chem. Phys.* **1989**, *91*, 3826.

(44) Zhou, M. F.; Hacaloglu, J.; Andrews, L. *J. Chem. Phys.* **1999**, *110*, 9450.

(45) Burkholder, T. R.; Andrews, L. *J. Chem. Phys.* **1991**, *95*, 8697.

(46) Hassanzadeh, P.; Andrews, L. *J. Phys. Chem.* **1992**, *96*, 9177.

(47) Zhou, M. F.; Andrews, L. *J. Am. Chem. Soc.* **1998**, *120*, 13230.

(48) *Gaussian 98, Revision A.1.* Frisch, M. J.; Trucks, G. W.; Schlegel, H. B.; Scuseria, G. E.; Robb, M. A.; Cheeseman, J. R.; Zakrzewski, J. A.; Montgomery, J. A.; Stratmann, R. E.; Burant, J. C.; Dapprich, S.; Millam, J. M.; Daniels, A. D.; Kudin, K. N.; Strain, M. C.; Farkas, O.; Tomasi, J.; Barone, V.; Cossi, M.; Cammi, R.; Mennucci, B.; Pomelli, C.; Adamo, C.; Clifford, S.; Ochterski, J.; Petersson, G. A.; Ayala, P. Y.; Cui, Q.; Morokuma, K.; Malick, D. K.; Rabuck, A. D.; Raghavachari, K.; Foresman, J. B.; Cioslowski, J.; Ortiz, J. V.; Stefanov, B. B.; Liu, G.; Liashenko, A.; Piskorz, P.; Komaromi, I.; Gomperts, R.; Martin, R. L.; Fox, D. J.; Keith, T.; Al-Laham, M. A.; Peng, C. Y.; Nanayakkara, A.; Gonzalez, C.; Challacombe, M.; Gill, P. M. W.; Johnson, B. G.; Chen, W.; Wong, M. W.; Andres, J. L.; Head-Gordon, M.; Replogle, E. S.; Pople, J. A. Gaussian, Inc., Pittsburgh, PA, 1998.

(49) Lee, C.; Yang, E.; Parr, R. G. *Phys. Rev. B* **1988**, *37*, 785.

(50) McLean, A. D.; Chandler, G. S. *J. Chem. Phys.* **1980**, *72*, 5639. Wachters, A. J. H. *J. Chem. Phys.* **1970**, *52*, 1033. Hay, P. J. *J. Chem. Phys.* **1977**, *66*, 4377. K. Raghavachari, K.; Trucks, G. W. *J. Chem. Phys.* **1989**, *91*, 1062.

(51) Peng, C.; Schlegel, H. B. *Isr. J. Chem.* **1994**, *33*, 449.

(52) Peng, C.; Ayala, P. Y.; Schlegel, H. B.; Frisch, M. J. *J. Comput. Chem.* **1996**, *17*, 49.

(53) Liang, B.; Andrews, L., to be published.

(54) Gabelnick, S. D.; Reedy, G. T.; Chasanov, M. G. *J. Chem. Phys.* **1974**, *60*, 1167.

Table 1. Infrared Absorptions (cm^{-1}) Observed for Reactions of Laser-Ablated Thorium with NO and O_2 in Excess Argon

$^{14}N^{16}O + ^{16}O_2$	$^{15}N^{16}O + ^{16}O_2$	$^{14}N^{16}O + ^{18}O_2$	identity
1589.3	1561.9	1561.9	$(NO)_2^+$
1458.3	1432.9	1452.6	***cis***-OONO$^-$
1433.3	1408.0	1426.2	***trans***-OONO$^-$
1243.7	1218.3	1218.3	NO_2^-
1222.7	1198.6	1198.6	***cis***-$(NO)_2^-$
1221.0	1199.9	1199.9	***trans***-$(NO)_2^-$
1039.5	1039.5	982.2	O_3
983.2	971.8	958.9	***trans***-OONO$^-$
981.1	981.1	926.6	$(O_2)_x(O_4^-)$?
978.3	978.3	924.7	$(O_2)_x(O_4^-)$?
953.8	953.8	901.7	O_4^-
879.0	879.0	832.0	ThO site
876.5	876.5	829.8	ThO
806.1	797.2	779.2	***cis***-OONO$^-$
805.2			O_3^- site
803.9			O_3^-
795.7	795.7	752.2	ThO_2 site
792.0	792.0	748.2	ThO_2 site
787.2	782.0	743.9	ThO_2
760.5	759.1	760.5	NThO
735.2	735.2	697.2	ThO_2
697.4	676.5	697.4	NThO
653.2	653.2	619.6	ThO_2^-

diatomic ThO oxygen 16/18 ratio, 1.0563, but close to the ratio 1.0545 for the antisymmetric mode in the ThO_2 molecule. This band split into a 1:2:1 triplet in the $^{16}O_2 + ^{16}O^{18}O + ^{18}O_2$ isotopic experiment but only a doublet feature in the $^{16}O_2 + ^{18}O_2$ experiment. The band is reduced to <10% on the addition of 0.05% CCl_4 to the sample,[37−40,57] which eliminated O_4^- and reduced ThO_2 by only 35%. We tentatively assign this band to the antisymmetric stretching mode in the ThO_2^- anion.

The second experiment involved the reaction between thorium and NO. Products bands include NThO at 760.5 and 697.4 cm^{-1},[1,58] and the metal-independent ionic products, ***cis***- and ***trans***-$(NO)_2^-$ at 1222.7 and 1220.9 cm^{-1}, NO_2^- at 1243.4 cm^{-1}, and $(NO)_2^+$ at 1589.2 cm^{-1}.[37,43]

Th + O_2/Ar + NO/Ar Experiments. In the reaction between laser-ablated thorium with O_2 and NO, metal-related bands, ThO, ThO_2, ThO_2^-, and NThO, and metal-independent bands, O_3, O_4^-, O_3^-, NO_2^-, $(NO)_2^-$, and $(NO)_2^+$, were again observed, as listed in the Table 1. Besides those absorptions common to the reaction between thorium and O_2 or NO, several new bands were observed. Figure 1 shows the 1480−1400-, 1000−940-, and 810−770-cm^{-1} regions from the infrared spectrum of a sample formed by laser-ablated thorium codeposited with 0.5% NO/Ar and 0.5% O_2/Ar at 7 K using an O_2 sample flow rate 50% higher than the NO sample. The bands at 1458.3 and 1433.3 cm^{-1} denoted as "c" and "t", respectively, were observed on deposition. A 25 K annealing slightly decreased the c-band, but did not change the t-band. Tungsten lamp irradiation increased the c-band by half, but decreased the t-band by half (Figure 1c) while O_4^- decreased 15%, ***cis***-$(NO)_2^-$ decreased 25%, and ***trans***-$(NO)_2^-$ increased 35%. Both new bands decreased on the following annealing to 35 K. Finally the c-band was totally eliminated, whereas the t-band was greatly decreased by 45 K annealing. A comparatively weaker band at 983.2 cm^{-1}, also denoted "t", tracks with the 1433.3-cm^{-1} band throughout the annealing and irradiation cycles and accounts for 5/8 relative absorption intensity. Weak nearby bands at 981.1 and 978.3 cm^{-1} (denoted "*") are common to laser ablation metal reactions with oxygen and are probably due to a higher order dioxygen anion cluster. Another new band at 806.1 (denoted "c") also tracks with the 1458.3-cm^{-1} band and is one-third of the relative absorption intensity.

Figure 2 shows spectra from laser-ablated thorium codeposited with 0.5% ^{15}NO/Ar and 0.5% O_2/Ar at 7 K. The 1458.3-cm^{-1} c-band shifted to 1432.9 cm^{-1}, with a nitrogen 14/15 isotopic ratio of 1.0177. The 1433.3-cm^{-1} t-band shifted to 1408.0 cm^{-1}, with a nitrogen 14/15 ratio of 1.0180. Both ratios are very close to the diatomic NO nitrogen 14/15 ratio of 1.0179, signifying that both absorptions arise from N−O stretching modes. The other t-band at 983.2 cm^{-1} shifted to 971.8 cm^{-1} in this experiment, and the other c-band absorption at 806.1 red-shifted to 797.2 cm^{-1}. The two lower bands have much smaller nitrogen 14/15 isotopic ratios, and are mixed vibrational modes. In the mixed ^{14}NO/^{15}NO + O_2 experiment, only three bands at 1458.4, 1433.1, and 1408.2 cm^{-1} were observed in the 1400−1500-cm^{-1} region (Figure 3f). However, the middle band is broader than both the 1433.3-cm^{-1} t-band in the ^{14}NO + O_2 experiment and the 1432.9-cm^{-1} c-band in the ^{15}NO + O_2 experiment, and clearly two absorptions contribute to this

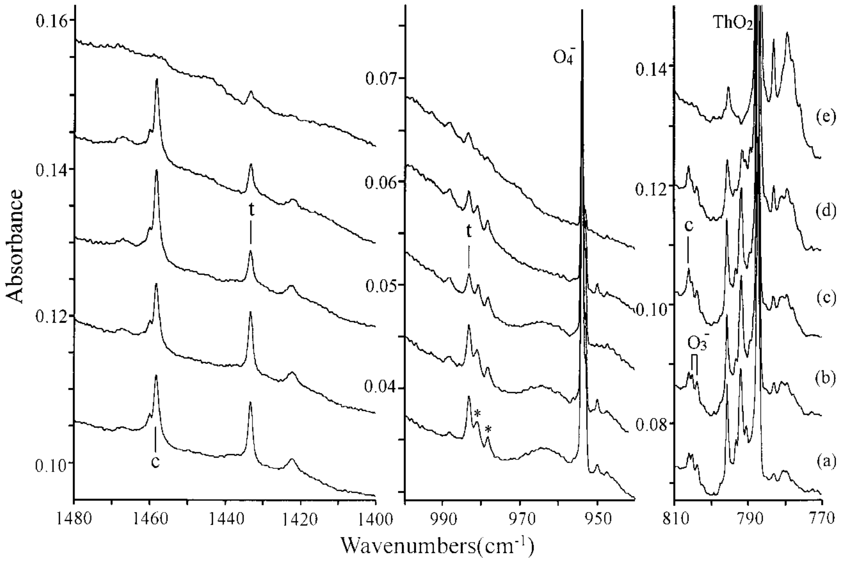

Figure 1. Infrared spectra in the 1480−1400-, 1000−940-, and 810−770-cm^{-1} regions for laser-ablated Th codeposited with 0.5% ^{14}NO in argon and 0.5% O_2 in argon at 7 K: (a) sample deposited for 70 min, (b) after 25 K annealing, (c) after 1-h W lamp irradiation, (d) after 30 K annealing, and (e) after 40 K annealing. The bands labeled "c" and "t" are identified in the text.

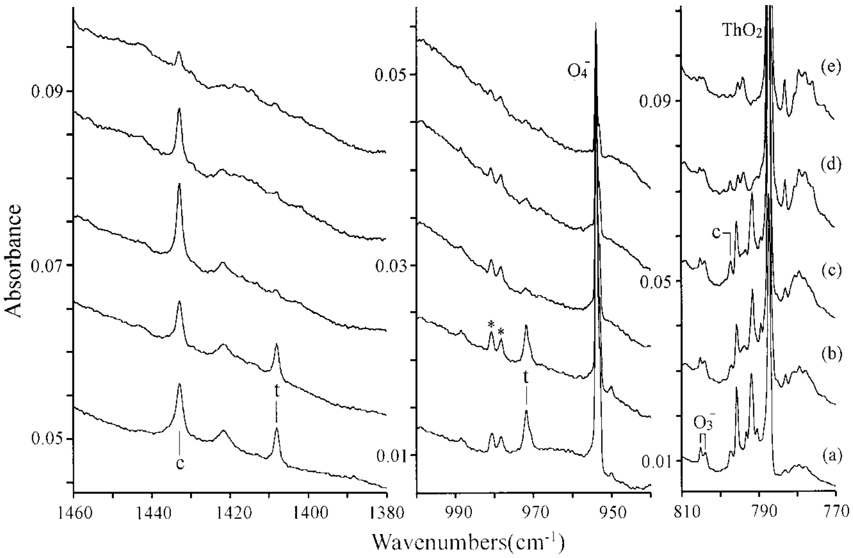

Figure 2. Infrared spectra in the 1460−1380-, 1000−940-, and 810−770-cm^{-1} regions for laser-ablated Th codeposited with 0.5% ^{15}NO in argon and 0.5% O_2 in argon at 7 K: (a) sample deposited for 70 min, (b) after 30 K annealing, (c) after 1-h W lamp irradiation, (d) after 35 K annealing, and (e) after 40 K annealing. The bands labeled "c" and "t" are identified in the text.

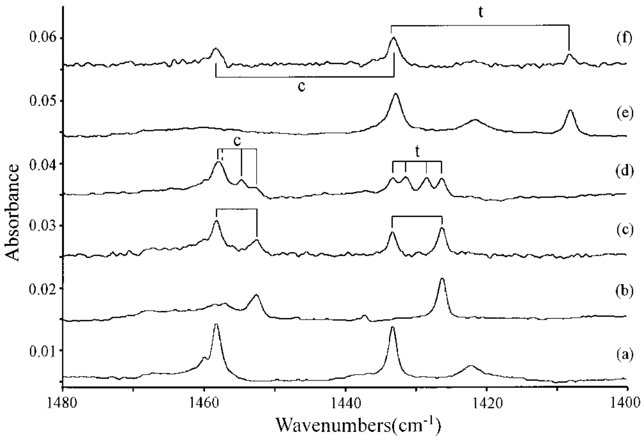

Figure 3. Infrared spectra in the 1480−1400-cm^{-1} region for laser-ablated Th codeposited with (a) 0.5% NO in argon and 0.5% O_2 in argon for 70 min, (b) 0.5% NO in argon and 0.5% $^{18}O_2$ in argon for 70 min, (c) 0.5% NO in argon and 0.4% $^{16}O_2$ + 0.4% $^{18}O_2$ in argon for 90 min, (d) 0.5% NO in argon and 0.13% $^{16}O_2$ + 0.26% $^{16}O^{18}O$ + 0.13% $^{18}O_2$ in argon for 90 min, (e) 0.5% ^{15}NO in argon and 0.5% O_2 in argon for 70 min, and (f) 0.25% ^{14}NO + 0.25% ^{15}NO in argon and 0.5% O_2 in argon for 80 min. The bands labeled "c" and "t" are identified in the text.

middle band. The isotopic splitting patterns for both c- and t-modes are doublets with two pure isotopic bands. The lower t- and c-counterparts also showed 1:1 doublet features at 983.2 and 971.8 cm^{-1} and at 806.1 and 797.2 cm^{-1}. These results reveal that there is only one NO subunit involved in the c- and t-absorbers.

In the reaction between thorium and NO/Ar + $^{18}O_2$/Ar, the 1458.3-cm^{-1} c-band red-shifted to 1452.6 cm^{-1} (Figure 3b); however, the lower c-band cannot be identified in this experiment, because of strong ThO_2 absorption. The t-bands red-shifted to 1426.2 and 958.9 cm^{-1}, respectively. In the NO + $^{16}O_2$/$^{18}O_2$ experiments, doublets were observed for both bands (Figure 3c). The c-doublet showed a relative intensity of 5:2, although equimolar concentrations of $^{16}O_2$ and $^{18}O_2$ were used. The lower t-band also showed a doublet at 983.2 and 958.9 cm^{-1}. In the NO + $^{16}O_2$/$^{16}O^{18}O$/$^{18}O_2$ (molar ratio 1:2:1) experiment (Figure 3d), the 1433.3-cm^{-1} t-band showed a 1:1:1:1 quartet splitting with new intermediate bands at 1431.4 and 1428.6 cm^{-1}. The lower t-band also split to a quartet with new bands at 976.9 and 963.2 cm^{-1}. The 1458.3-cm^{-1} c-band split into a triplet at 1458.1, 1454.8 and 1452.7 cm^{-1}, with approximate relative intensity of 4:2:1. Compared to the relative intensities of the 1458.3- and 1452.6-cm^{-1} bands in the previously mentioned NO + $^{16}O_2$/$^{18}O_2$ reaction (Figure 3c), this 1458.1-cm^{-1} band clearly contains more than one absorption. The overall splitting pattern of this 1458.3-cm^{-1} c-band in the scrambled oxygen experiment should also be a quartet. The isotopic splitting pattern of the lower c-band (806.1-cm^{-1}) cannot be resolved. The 1458.3- and 1433.3-cm^{-1} bands showed small $^{18}O_2$ isotopic shifts (5.7 and 7.1 cm^{-1}, respectively), indicating that both N−O stretching modes are slightly coupled with the oxygen molecule. The doublet feature in the $^{16}O_2$/$^{18}O_2$ mixture, and the quartet feature in the $^{16}O_2$/$^{16}O^{18}O$/$^{18}O_2$ mixture, indicate that there is one oxygen molecule involved in the responsible molecules, and the two oxygen atoms in this oxygen molecule are not equally involved in the 1458.3- and 1433.3-cm^{-1} modes.

CCl_4 is well known for its electron capture ability, and it has been used in this laboratory to help identify numerous ionic species.[37−40,57] The 0.5% O_2 argon sample was doped with 0.05% CCl_4, the experiment with laser-ablated thorium and 0.5% NO/Ar mixture was repeated, and the c-, t-, O_4^-, and $(NO)_2^-$ absorptions were not observed. This result suggests that both c- and t-absorbers are anionic species. Finally, codepositing 0.5% O_2 and 0.5% NO in argon onto a 7 K CsI substrate gave no product bands except for a small amount of NO_2, which is similar to a previous study.[59]

Other Metals + O_2/Ar + NO/Ar. Nine other metals, Al, Fe, In, Li, Ni, Pd, Ru, Tl, and Y, were ablated with various isotopic O_2 + NO samples to demonstrate the metal-independent character of the c- and t-bands. Except for thallium, where a very strong TlNO absorption at 1454.6 cm^{-1} masked this region,[60] all other metals showed absorptions at 1458.3 ± 0.1

---

(55) Andrews, L.; Spiker, R. C., Jr. *J. Phys. Chem.* **1972**, *76*, 3208.
(56) Andrews, L.; Ault, B. S.; Grzybowski, J. M.; Allen, R. O. *J. Chem. Phys.* **1975**, *62*, 2461.
(57) Zhou, M. F.; Andrews, L. *J. Am. Chem. Soc.* **1998**, *120*, 11499.
(58) Kushto, G. P.; Andrews, L. *J. Phys. Chem. A* **1999**, *103*, 4836.
(59) Andrews, L.; Hassanzadeh, P.; Brabson, G. D.; Citra, A.; Neurock, M. *J. Phys. Chem.* **1996**, *100*, 8273.
(60) Zhou, M. F.; Andrews, L. *J. Phys. Chem. A* **2000**, *104*, 8475.

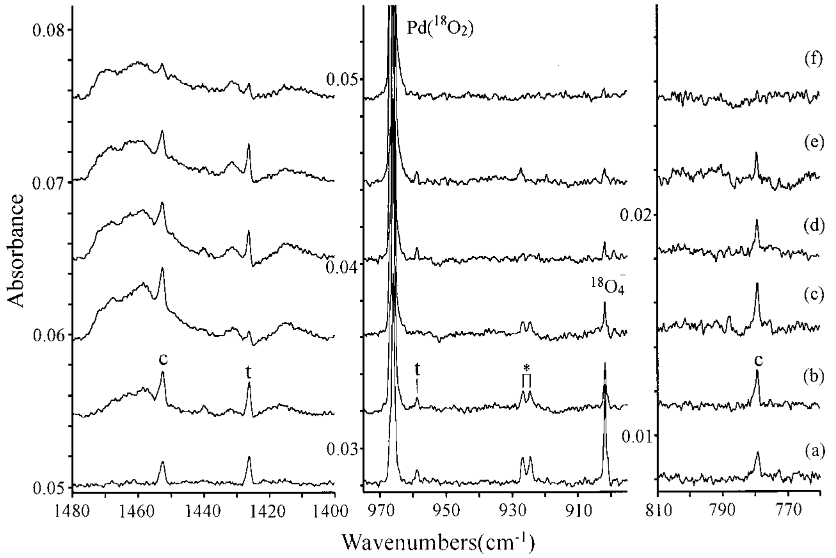

Figure 4. Infrared spectra in the 1480−1400-, 975−895-, 810−760-cm^{-1} regions for laser-ablated Pd codeposited with 0.5% NO in argon and 0.2% $^{18}O_2$ in argon at 7 K: (a) sample deposited for 90 min, (b) after 1-h $\lambda > 290$-nm irradiation, (c) after 1-h W lamp irradiation, (d) after 40-min $\lambda > 290$-nm irradiation, (e) after 30 K annealing, and (f) after 40-min $\lambda > 240$-nm irradiation.

and 1433.3 ± 0.1 cm^{-1}. Although the lower t- and c-bands are weaker, they were observed in all but the nickel experiment, where strong oxide bands are dominant. All c- and t-bands in different metal and isotopic experiments showed no metal dependence as their absorption wavenumbers differ from the values in Table 1 by no more than 0.1 cm^{-1}.

Figure 4 shows the 1480−1400-, 975−895-, and 810−760-cm^{-1} region for laser-ablated palladium with NO and $^{18}O_2$ in argon. The strong absorption at 966.0 cm^{-1} is due to Pd($^{18}O_2$).[61] The intensities of both t- and c-bands are not as strong as in the thorium experiment (Figure 3b), and a reduced yield was also observed for the $^{18}O_4^-$ band at 901.7 cm^{-1}.[36] One advantage of this experiment is the clean region around 800 cm^{-1}, in contrast to strong dioxide bands in the thorium experiment. In this palladium experiment, we can identify the ^{18}O-substituted lower c-band at 779.2 cm^{-1}. Figure 4a shows the spectrum after sample deposition; $\lambda > 290$ nm irradiation (Figure 4b) increased both c- and t-bands, and a following tungsten lamp irradiation increased c by a third, and eliminated t. Another $\lambda > 290$-nm irradiation almost restored both bands to the level before the tungsten lamp irradiation. A subsequent 30 K annealing decreased c-bands, and increased t-bands slightly, and a full-arc irradiation eliminated all t- and c-bands.

Figure 5 illustrates the 1480−1400-cm^{-1} region of laser-ablated iron codeposited with 0.5% NO in argon + 0.15% $^{16}O_2$ and 0.25% $^{18}O_2$ in argon to explore different photochemistry. First, irradiation using a tungsten lamp increased the c-bands by half and almost destroyed the t-bands (Figure 5c) and decreased $(NO)_2^-$ bands by a third. Then a following $\lambda > 290$-nm mercury-arc irradiation decreased c-bands by a third, but recovered almost half of t-bands from the last annealing. A full arc $\lambda > 240$-nm irradiation decreased both c- and t-bands, and the last annealing to 35 K almost eliminated these bands.

Finally, Figure 6 illustrates a Ru experiment with NO and O_2 to contrast the photochemistry of NO_2^-, $(NO)_2^-$, O_4^-, and the new product species. Annealing to 25 K has little effect on the product features. Visible−near-infrared photolysis clearly increases the c-feature and decreases the t-absorption, but O_4^- and trans $(NO)_2^-$ also decrease (Figure 6c). A subsequent $\lambda >$ 290-nm exposure decreases the c, ***cis***-$(NO)_2^-$, and O_4^- bands and increases the t absorptions (Figure 6d), but final exposure to the full arc decreases all of these features (Figure 6e).

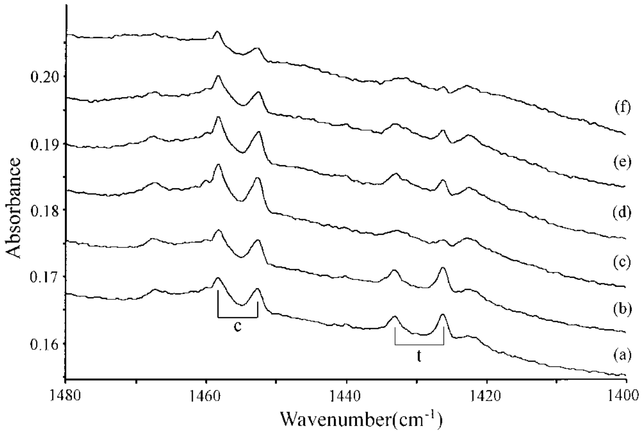

Figure 5. Infrared spectra in the 1480−1400-cm^{-1} region for laser-ablated Fe codeposited with 0.5% NO in argon and 0.15% $^{16}O_2$ + 0.25% $^{18}O_2$ in argon at 7 K: (a) sample deposited for 90 min, (b) after 25 K annealing, (c) after 1-h W lamp irradiation, (d) after 1-h $\lambda > 290$-nm irradiation, (e) after 30-min $\lambda > 240$-nm irradiation, and (f) after 35 K annealing.

Calculations. DFT calculations using the B3LYP functional and 6-311+G(d) basis set for both ***cis***- and ***trans***-$OONO^-$ and the transition state have been reported previously.[19] These results were reproduced, and in addition, infrared intensities and isotopic frequencies were computed as listed in the Table 2. In short, ***cis***-$OONO^-$ is more stable than ***trans***-$OONO^-$ by 3.0 kcal/mol, and each isomer has several frequencies with sufficient infrared intensity to be observed. For comparison, calculations using the BPW91 functional gave lower frequencies closer to the observed values as expected.

Identification of c- and t-Absorbers. Doublet splitting patterns were observed for all c- and t-bands in the mixed ^{14}NO/^{15}NO experiment, and hence, it is obvious that only one NO unit is involved in both c- and t-products. In the mixed $^{16}O_2$/$^{18}O_2$ experiment, doublet splitting features were observed, whereas in the $^{16}O_2$/$^{16}O^{18}O$/$^{18}O_2$ experiment, quartets were observed for 1458.3- and 1433.3-cm^{-1} bands. This demonstrates

---

[61] Bare, W. D.; Citra, A.; Chertihin, G. V.; Andrews, L. *J. Phys. Chem. A* **1999**, *103*, 5456 and references therein.

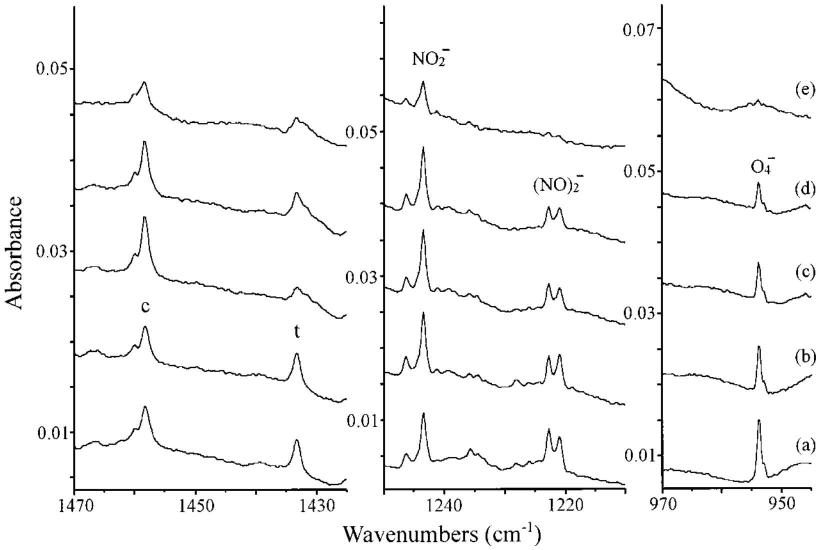

Figure 6. Infrared spectra in the 1470−1425-, 1250−1210-, 970−945-cm^{-1} regions for laser-ablated Ru codeposited with 0.5% NO in argon and 0.5% O_2 in argon at 7 K: (a) sample deposited for 70 min, (b) after 25 K annealing, (c) after 1-h W lamp irradiation, (d) after 1-h $\lambda > 290$-nm irradiation, and (e) after 40-min $\lambda > 240$-nm Hg lamp irradiation.

Table 2. Ground Electronic States, Equilibrium Geometries, Relative Energies, and Isotopic Frequencies Calculated for ***cis***-$OONO^-$, ***trans***-$OONO^-$, and Their Transition State (TS)[a]

		frequencies, cm^{-1} (infrared intensities)						
species	geometries (Å, deg)	isotopic molecule	OON bend	OONO tors	O−N str	O−O str	ONO bend	N=O str
c-$OONO^-$	O−O, 1.388; O−N, 1.367;	16−16−14−16	336.4	496.9	718.1	833.9	969.2	1517.0
$^1A'$	N=O, 1.213; ∠OON, 118.3;		(3)	(0)	(34)	(160)	(19)	(395)
	∠ONO, 116.3; D(OONO), 0.0	16−16−15−16	336.3	489.5	711.3	822.2	964.1	1489.1
		18−18−14−16	325.4	484.7	688.9	808.4	933.6	1516.7
t-$OONO^{-b}$	O−O, 1.408; O−N, 1.338;	16−16−14−16	422.6	256.1	852.0	627.1	1024.4	1489.2
$^1A'$	N=O, 1.228; ∠OON, 114.1;		(12)	(7)	(0)	(25)	(324)	(360)
	∠ONO, 111.2; D(OONO), 180.0	16−16−15−16	419.6	253.7	846.8	623.8	1011.3	1461.1
		18−18−14−16	407.2	249.6	811.1	608.6	998.9	1486.1
TS[b]	O−O, 1.501; O−N, 1.417;	16−16−14−16	270.1	620.5i	574.5	756.0	822.6	1609.3
^1A	N=O, 1.191; ∠OON, 114.1;		(15)	(8)	(42)	(31)	(132)	(345)
	∠ONO, 101.8; D(OONO), 77.3							

[a] DFT/B3LYP calculation, 6-311+G(d) on N, O. [b] Relative energy (including zero-point energy) compared to ***cis***-$OONO^-$ is 3.0 and 25.8 kcal/mol for ***trans***-$OONO^-$ and the transition state, respectively. The higher energy triplet state is a weak complex of NO and O_2^-; see ref 19.

the involvement of one oxygen molecule in both c- and t-absorbers, with the two oxygen atoms not participating equally in the vibrational modes. Hence, both c- and t-absorbers involve single O_2 and NO molecules. The c- and t-bands were not observed in the experiment without laser ablation or in the CCl_4 doped experiment, which suggests the anion identification for both c- and t-absorbers.

The DFT/B3LYP calculation predicted strong infrared bands for ***cis***-$OONO^-$ at 1517.0 and 833.9 cm^{-1}, with intensities of 395 and 160 km/mol, respectively, and for ***trans***-$OONO^-$ at 1489.2 and 1024.4 cm^{-1}, with intensities of 360 and 324 km/mol, respectively. Excellent agreement with the experimental result identifies the c-absorber as ***cis***-$OONO^-$; the two observed modes at 1458.3 and 806.1 cm^{-1} require scale factors of 0.961 and 0.967, which are expected values for DFT/B3LYP calculations.[62] The t-absorber is assigned as ***trans***-$OONO^-$, and the two observed modes at 1433.3 and 983.2 cm^{-1} require scale factors of 0.962 and 0.960. The calculated intensities of two modes in ***trans***-$OONO^-$ do not fit the experimental data as well as in ***cis***-$OONO^-$, but the predicted trends are correct. The vibrational frequencies for isotopic species agree with the experimental data, except for overestimation of the ^{15}N shift and underestimation of O_2 involvement in the terminal N=O stretching mode. For example, the B3LYP computation predicts a $^{14}N^{16}O/^{15}N^{16}O$ frequency ratio 1.0187 for cis and 1.0192 for trans and the observed ratios are 1.0177 and 1.0180, respectively. The calculation predicts a 0.3-cm^{-1} $^{18}O_2$ shift for cis and 3.1 cm^{-1} for trans, but 5.7 and 7.1 cm^{-1}, respectively, are observed.

The stable ***cis***-$OONO^-$ and ***trans***-$OONO^-$ anions separated by a substantial 25.8 kcal/mol energy barrier are both observed isolated in the matrix independent of the metal cation that provided the anion electron. Likewise, both alkali metal-dependent $(M^+)(OONO^-)$ conformers are produced by photolysis of MNO_3 "molecules" in solid argon;[25] however, the normal modes in the $(M^+)(OONO^-)$ isomers involve the alkali cation to a minor degree. In contrast, interactions in the tetramethylammonium peroxynitrite crystalline solid apparently favor the cis form.[20]

We have found no evidence for the isolated NO_3^- anion, observed at 1356 cm^{-1} in solid neon,[63] or the nitrate radical, observed at 1492 cm^{-1} in the gas phase.[64] Apparently, ultraviolet photolysis dissociates or detaches isolated $OONO^-$ before

---

(62) Bytheway, I.; Wong, M. W. *Chem. Phys. Lett.* **1998**, *282,* 219.

rearrangement can occur, in contrast to that observed for the ion-pair (M^+)($OONO^-$) species.[25]

Mechanistic Considerations. Two possible reaction channels can participate in the matrix experiment to produce the isolated ***cis***-$OONO^-$ and ***trans***-$OONO^-$ anions, namely, O_2^- reacting with NO or NO^- reacting with O_2. Electrons produced in the laser ablation process are captured by NO and O_2 as attested by observation of their dimer anions from reactions 1 and 2

$$NO^- + NO \rightarrow (NO)_2^- \quad (1)$$

$$O_2^- + O_2 \rightarrow O_4^- \quad (2)$$

$$O_2^- + NO \rightarrow OONO^- \quad (3)$$

$$NO^- + O_2 \rightarrow OONO^- \quad (4)$$

$$NO^- + O_2 \rightarrow O_2^- + NO \quad (5)$$

as demonstrated in several recent investigations,[36,37,42,43] although $(NO)_2^-$ can also be formed through electron capture by $(NO)_2$. Accordingly, O_2^- can react with NO, and on the other hand, NO^- can combine with O_2, to give $OONO^-$, reactions 3 and 4, in both stable cis and trans forms. Since fast electron transfer has been observed between NO^- and O_2, reaction 5,[26−28] reaction 3 probably dominates the yield of $OONO^-$ anions in these experiments. Owing to numerous argon collisions with NO^- and O_2^- during condensation, the more stable O_2^- anion[65] is expected to have a higher survival rate since in the gas phase reaction 5 dominates.[26−28] Argon collisions with $OONO^-$ during condensing the argon matrix appear to be crucial to stabilization of the dimer anion complex product of reaction 3.

Reactions 3 and 4 are elementary processes, and an increase in either NO or O_2 concentration should increase the reaction rate and yield of product. However, note that NO undergoes a dimerization reaction, but O_2 does not, and the electron (and anion) concentration is the limiting reagent as anion absorptions in these experiments are typically a few percent as intense as corresponding neutral absorptions. We find that doubling the NO concentration from 0.25 to 0.5% while maintaining the other experimental conditions has no effect on the $OONO^-$ absorptions. However, doubling the O_2 concentration increased the cis and trans product bands by 75%, and doubling the flow rate of the O_2/Ar sample almost doubled the product absorptions. This evidence, we believe, supports the hypothesis that the formation of O_2^- is the rate-determining step and that reaction 3 is the dominant mechanism in these experiments.

Photochemical isomerization was observed between the ***cis***- and ***trans***-peroxynitrite anions. Visible and near-infrared radiation from a reduced intensity tungsten lamp decreased trans and increased cis absorptions (Figures 4−6) whereas a subsequent exposure to ultraviolet−visible mercury arc light reduced the cis and almost reproduced the trans isomer. This reversible isomerization reaction proceeds through rotation of the middle N− O bond. The transition state is 25.8 kcal/mol higher in energy than the ***cis***-$OONO^-$ isomer. This activation barrier suggests significant conjugation of π symmetry orbitals across the central N−O bond. An 800-nm photon provides enough energy to overcome this barrier. A subsequent $\lambda > 240$-nm irradiation reduced both isomers and failed to give evidence for NO_2^- or NO_3^-. As has been observed in several matrix photoisomerism processes including $(S_2)_2$ and $(Te_2)_2$, excitation of one isomer into a dynamically equilibrating state allows the isomer not absorbing light to be relaxed and stabilized by the cold matrix.[66,67] Similar results have been reported for the (K^+)($OONO^-$) isomers in solid argon.[25] Irradiation at 308 nm decreased cis and enhanced trans, but prolonged irradiation reduced the trans isomer in favor of the original KNO_3 form.

$$\textbf{\textit{cis}}\text{-}OONO^- \underset{\text{vis, near-IR}}{\overset{\text{near-UV, vis}}{\rightleftarrows}} \textbf{\textit{trans}}\text{-}OONO^-$$

Conclusions

Laser ablation of 10 different metal targets with concurrent 7 K codeposition of NO/Ar and O_2/Ar mixtures produces new metal-independent bands at 1458.3 and 806.1 cm^{-1} and at 1433.3 and 983.2 cm^{-1}. These absorptions require both O_2 and NO. Furthermore, the product bands were not observed in a CCl_4 doped sample due to electron capture by CCl_4 or in an O_2 and NO experiment without laser ablation to provide electrons, which identifies anion products. Based on the isotopic shifts, the splitting patterns in the mixed isotopic experiments, these anions require one NO and one O_2 molecule. On comparison with DFT/B3LYP calculations, the former (1458.3 and 806.1 cm^{-1}) bands are assigned to ***cis***-$OONO^-$, and the latter (1433.3 and 983.2 cm^{-1}) bands are assigned to ***trans***-$OONO^-$. The present metal-independent ***cis***- and ***trans***-$OONO^-$ absorptions are near the ***cis***- and ***trans***-MOONO (M = K, Na, Li) absorptions,[25] where the latter bands showed significant shifts with different alkali metals.

Both ***cis***- and ***trans***-$OONO^-$ isomers observed in the current experiments are probably formed by the ion−molecule reaction between O_2^- and NO, which can access the stable minima on each side of the barrier between them. A reversible photoisomerism has been found in the solid argon matrix with visible and near-ultraviolet radiation, but $\lambda > 240$-nm light destroys both isomers.

Acknowledgment. The authors gratefully acknowledge National Science Foundation support under grant CHE 00-78836.

JA0114299

---

(63) Forney, D.; Thompson, W. E.; Jacox, M. E. *J. Chem. Phys.* **1993**, *99*, 7393.

(64) Ishiwata, T.; Tanaka, I.; Kawaguchi, K.; Hirota, E. *J. Chem. Phys.* **1985**, *82*, 2196.

(65) Travers, M. J.; Cowles, D. C.; Ellison, G. B. *Chem. Phys. Lett.* **1989**, *164*, 449.

(66) Hassanzadeh, P.; Andrews, L. *J. Phys. Chem.* **1992**, *96*, 6579.

(67) Hassanzadeh, P.; Thompson, C.; Andrews, L. *J. Phys. Chem.* **1992**, *96*, 8246.